CHAPTER 5

Characterization of poorly-immunodepleted peaks and identified PLA_2 enzymes from *B. fasciatus* venom of Assam, India

Chapter 5

Characterization of poorly-immunodepleted proteins and identified PLA$_2$ enzymes from *B. fasciatus* venom of Assam, India

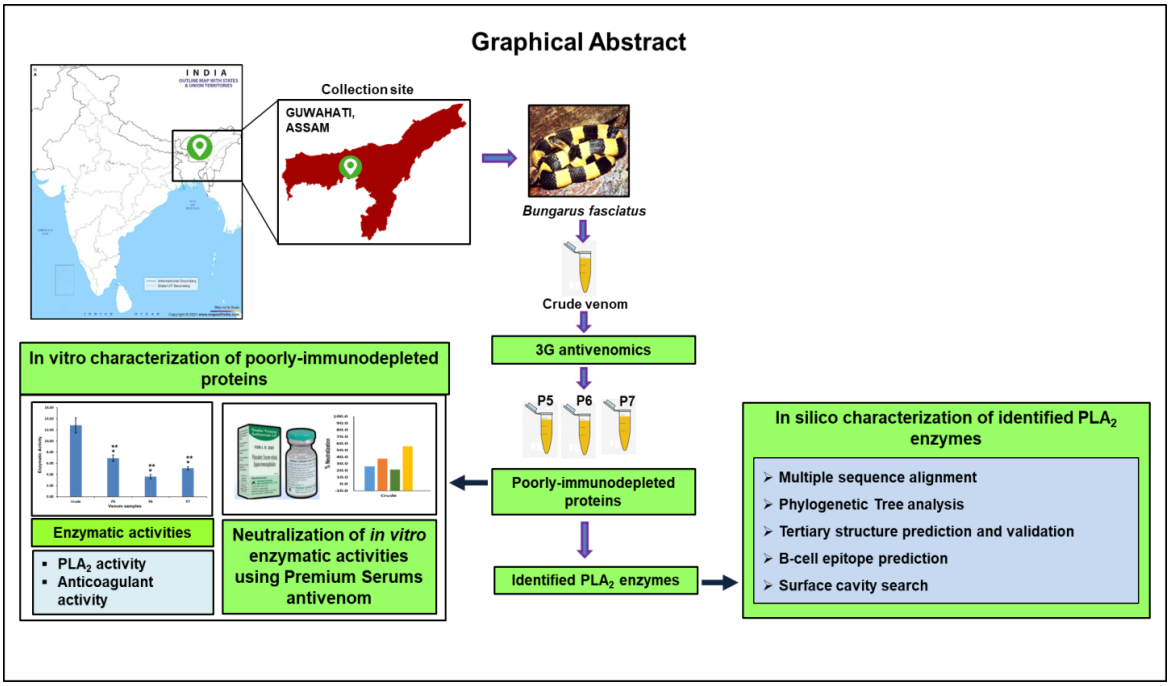

5.1 Introduction

Snake venom PLA$_2$ enzymes may share similarity in their primary, secondary and tertiary structure, however, they vary widely in inducing their pharmacological effects [237]. The PLA$_2$ enzymes generally lack a direct hemolytic activity [238], however, addition of external phospholipids may produce indirect hemolytic activity due to the production of lytic hydrolysis products [169]. Some of the PLA$_2$ enzymes may exhibit pre-synaptic neurotoxicity where they target the nerve termini, whereas some others may exhibit post-synaptic neurotoxicity where they mostly target the muscle cells. Myotoxicity induced by PLA$_2$ enzymes may induce both local myonecrosis or systemic myotoxicity, which leads to the extrusion of creatine phosphokinase (CPK) in the victim's plasma [239,240]. Some PLA$_2$ enzymes have exhibited direct cardiotoxic effects on the cardiovascular system, which is due to membrane lysis caused by enzymes

and is independent of the enzymatic activity [241,242]. PLA_2s from *Naja nigricollis* and *Ophiophagus hannah* have been reported to induce intracellular structural modifications and contracture [234,243,244]. PLA_2 enzymes commonly exhibit anticoagulant property and these enzymes can be grouped as strongly-anticoagulant, weakly-anticogulant or non-anticoagulant depending on the dosage required for the activity [235,245]. Moreover, PLA_2 enzymes also exhibit platelet aggregation or inhibition activity [246,247], edema inducing activity [248], induction of myoglobinuria [249] as well as antimicrobial effects [237,250].

Antivenom cross-reactivity at the molecular level is dependent on the recognition sites (epitopes) on snake venom toxins**.** These sites need not necessarily be the active site of the toxins rather it may also be sites for allosteric inhibition or sites which interact with the target tissue. Although information on these interactions is limited, identification of these sites and understanding their interactions with the antibody may explain the immunological limitations of existing antivenom [251]. Immunization of animals like horses during antivenom manufacturing is a complex and challenging task due to the use of toxic and lethal venom toxins as immunogens. Use of non-toxic synthetic peptides corresponding to the epitopes of the venom toxins can also be explored for the development of effective antivenom or vaccines [252,253]. As an alternative to antivenom, inhibitors such as repurposed drugs, small synthetic inhibitors, synthetic nanoparticles and oligonucleotide aptamers are explored to study their efficacy in inhibition of venom proteins [102,105,109]. In this context, *in silico* studies become extremely useful to screen such molecules from large libraries and also help in designing appropriate inhibitors corresponding to the binding site. Identification of the surface cavity which lies in close vicinity of the active site or allosteric site plays a crucial role in this aspect.

In this chapter, the in vitro enzymatic activities of the poorly-immunodepleted PLA_2 proteins have been studied. Moreover, the seven identified PLA_2 enzymes were compared with known PLA_2 enzymes from representatives of "Big-Four" snakes (*B. caeruleus* and *D. russelii*) using multiple sequence alignment and phylogenetic tree analysis. Finally their tertiary structures were predicted, and the B-cell epitopes and surface cavity on the PLA_2 enzymes have also been predicted and compared.

5.2 Methods

5.2.1 Characterization of poorly-immunodepleted PLA_2 proteins

5.2.1.1 PLA_2 activity

The crude venom and P5, P6 and P7 peaks were subjected to PLA_2 activity assay (1 µg/ml) using the $sPLA_2$ assay kit (colorimetric method) described previously in chapter 2 (section 2.3.4).

5.2.1.2 Anticoagulant activity

Prothrombin Time (PT), Activated Partial Thromboplastin Time (APTT) and Recalcification Time (RT) of *B. fasciatus* venom and P5, P6 and P7 peaks (10 µg/ml) were determined using the methodology mentioned in chapter 2 (section 2.3.5).

5.2.2 Neutralization of enzymatic activities by polyvalent antivenom manufactured in India

In vitro neutralization of PLA_2 activity for *B. fasciatus* venom and poorly-immunodepleted (P5, P6 and P7) peaks was tested by taking 1 µg sample and then adding 100 µg of polyvalent antivenom (Premium Serums) at 1:100 ratio. The mixture was incubated for 1 h at 37 ^oC and residual PLA_2 activity utilizing the method outlined in chapter 2 (section 2.3.4). The negative control comprised *B. fasciatus* venom combined with assay buffer.

For neutralization of anticoagulant property, the *B. fasciatus* venom and P5, P6 and P7 peaks (10 µg) was incubated with 1000 µg of the antivenom at 1:100 ratio for 1 h at 37 ^oC. Post incubation, samples from the mixture was taken to determine the RT, PT and APTT using the method previously outlined in chapter 2 (section 2.3.5). For negative control, PPP along with assay buffer was taken, and the positive control involved a mixture of crude venom and PPP.

5.2.3 Multiple sequence alignment

Utilizing the 'BLASTp' server (https://blast.ncbi.nlm.nih.gov/Blast.cgi?PAGE=Proteins) of the NCBI (National Center for Biotechnology Information) database, the amino acid sequences of the seven identified PLA_2 enzymes were retrieved. Multiple sequence alignment of the PLA_2 enzymes was carried out using DNAMAN X (version 10.3.6.158)

and 'Percent identity matrix' was obtained from online tool 'Clustal Omega' version 1.2.4 (https://www.ebi.ac.uk/Tools/msa/clustalo/). The secondary structure prediction of the identified PLA_2 enzymes was performed in PROTEUS structure prediction tool 2.0 (http://www.proteus2.ca/proteus2/).

5.2.4 Phylogenetic tree analysis

A phylogenetic tree of the identified seven poorly-immunodepleted PLA_2 enzymes with other known PLA_2s of the "Big-Four" snakes of India was constructed utilizing the neighbour-joining algorithm in MEGA software (v11.0). The number of bootstrap replications was taken as 1000 and the substitution model chosen was the Poisson method.

5.2.5 Tertiary structure prediction using Homology modelling and its validation

The primary sequence of the identified seven poorly-immunodepleted PLA_2 enzymes obtained from NCBI database using 'BLASTp' was utilized to obtain homology structure of the enzymes utilizing tertiary structure modelling in SWISS-MODEL-Expasy server (https://swissmodel.expasy.org/). Based on the Sequence identity and Global Model Quality Estimate (GMQE) a template was selected from the following three: Phospholipase A_2 BF-16 (B2KNL1), Acidic phospholipase A_2 KBf-grIB (P0C551) and Neutral Phospholipase A_2 3 (P1461). The models were visualized using the software Biovia Discovery Studio Visualizer v21.1.0.20298. Validation of the homology model for quality was done based on GMQE, MolProbity score, Clash score, Ramachandran Plot and ERRAT overall quality factor. The GMQE was obtained while selecting templates in SWISS-MODEL Expasy. MolProbity score and Clash score were obtained from Duke University School of Medicine website (http://molprobity.biochem.duke.edu/). The MolProbity score is an overall score which reflects the 'goodness' of a structure taking into account the bond angles, bond length, torsion angles and steric clashes. Typically a score below 2.0 is considered good for structures below 2.0 Å resolution. Clash score typically measures the number of steric clashes per 1000 atoms in the protein structure and typically a clash score between 0 to 10 is preferred. Ramachandran plot analysis was obtained from PROCHECK program at SAVES version 6.0 server (https://saves.mbi.ucla.edu/). Understanding how the peptides are distributed in the permitted and non-permitted regions of the Ramachandran plot

helps to assess the accuracy of the predicted models. The non-bonded atomic interactions of the model are analysed using the ERRAT program (SAVES v6.0 server). The 'Overall quality factor' of the predicted structures was determined in the program, where a value of ≥95% is considered a good structure with a high resolution. Energy minimization of a PLA_2 enzyme was done using the ModRefiner server (https://zhanggroup.org/ModRefiner/) for refinement of protein-structure at a high-resolution.

5.2.6 B-cell epitope prediction of identified PLA_2 enzymes

For the prediction of linear B-cell epitopes in the identified seven poorly-immunodepleted PLA_2 enzymes BepiPred 2.0 (https://services.healthtech.dtu.dk/services/BepiPred-2.0/) web server was utilized. BepiPred 2.0 is trained to identify epitopes from antigen-antibody structures using a random forest algorithm. The default epitope threshold of 0.5 was used to identify the epitopes. The discontinuous or conformational B-cell epitopes were predicted in the Ellipro webserver (http://tools.iedb.org/ellipro/). The predicted 3D structure of identified PLA_2 enzymes by homology modelling was used as the input protein structure. Ellipro provides a Protrusion index score (Ellipro score) where a higher score indicates a greater solvent accessibility. The allergenicity of the predicted epitopes was determined using AllerCatPro 2.0 (https://allercatpro.bii.a-star.edu.sg/allergy/index.html). AllerCatPro 2.0 predicts the amino acid and structural similarly of input sequence to 5306 allergens which include protein allergens as well as autoimmune allergens from various databases [254]. The helical content of both linear and conformational B-cell epitopes was calculated using the Agadir tool (http://agadir.crg.es/).

5.2.7 Surface cavity search

Surface cavity search for the predicted proteins models was performed utilizing the CASTp 3.0 server (http://sts.bioe.uic.edu/castp/index.html?201l) previously described by Tian et al. [255].

5.2.8 Statistical analysis

Statistical significance of the obtained values for in vitro assays was calculated by One-Way ANOVA analysis using Microral Origin software v6.0. The significance level was designated by their respective *p*-values ($^{\#}p<0.001$, $^{**}p<0.01$ and $^{*}p<0.05$).

5.3 Results

5.3.1 Characterization of poorly-immunodepleted PLA_2 proteins

5.3.1.1 PLA_2 activity

The PLA_2 activity of the crude *B. fasciatus* venom and poorly-immunodepleted proteins was determined in terms of specific activity (µmol/min/ml/µg) (Figure 5.1). The activity was highest for the crude venom sample (12.8 ± 1.4). This was followed by the peaks P5 (6.9 ± 0.6) (**p<0.01), P7 (5.1 ± 0.3) ($^{\#}p$<0.001) and P6 (3.6 ± 0.4) ($^{\#}p$<0.001).

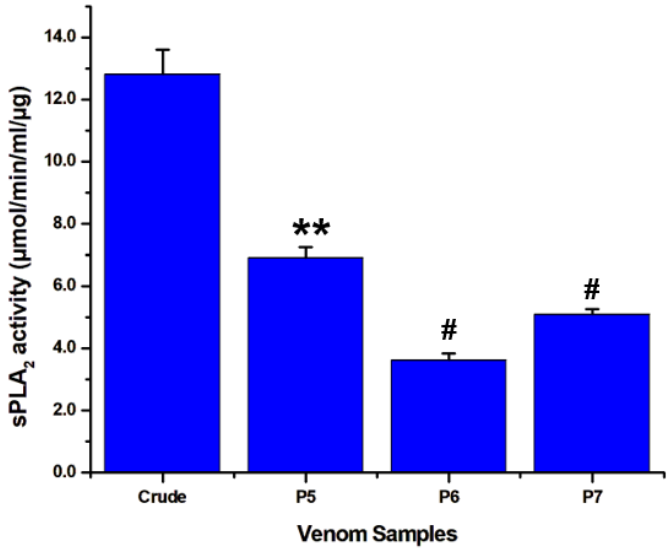

Figure 5.1: $sPLA_2$ activity of *B. fasciatus* venom and poorly-immunodepleted P5, P6 and P7 peaks from Guwahati, Assam. The activity was represented in µmol/min/ml/µg. Each bar depicts the mean ± S.E of three distinct experiments. The significance level (**p<0.01 and $^{\#}p$<0.001) is in relation to the crude venom.

5.3.1.2 Anticoagulant activity

The anti-coagulant effect of the crude venom from *B. fasciatus* as well as poorly-immunodepleted proteins was determined. In RT, the NCT (186.6 ± 14.7 s) of PPP was delayed to 135.7 s by the crude venom (322.3 ± 29.4 s). The peaks also exhibited anticoagulant effect and delayed the NCT [P5 (305.3 ± 0 s), P7 (254.5 ± 25.4 s) and P6 (212.0 ± 14.7 s)]. In PT, the NCT (11.3 ± 1.2 s) was delayed to the highest extent by P7 (24.0 ± 3.7 s) and P5 (24.0 ± 2.0 s) followed by P6 (22.7 ± 3.1 s) and crude venom (18.7 ± 3.1 s) respectively. Further, in APTT, the NCT (58.6 ± 4.4 s) was delayed and the highest anticoagulant effect was demonstrated by P5 (135.1 ± 11.7 s), followed by crude

(130.0 ± 7.7 s), P7 (107.1 ± 7.7 s) and P6 (102.0 ± 4.4 s) respectively. The statistically significant difference of the peaks when compared to the crude venom are represented by the *p*-value (*p<0.05 and **p<0.01) (Figure 5.2).

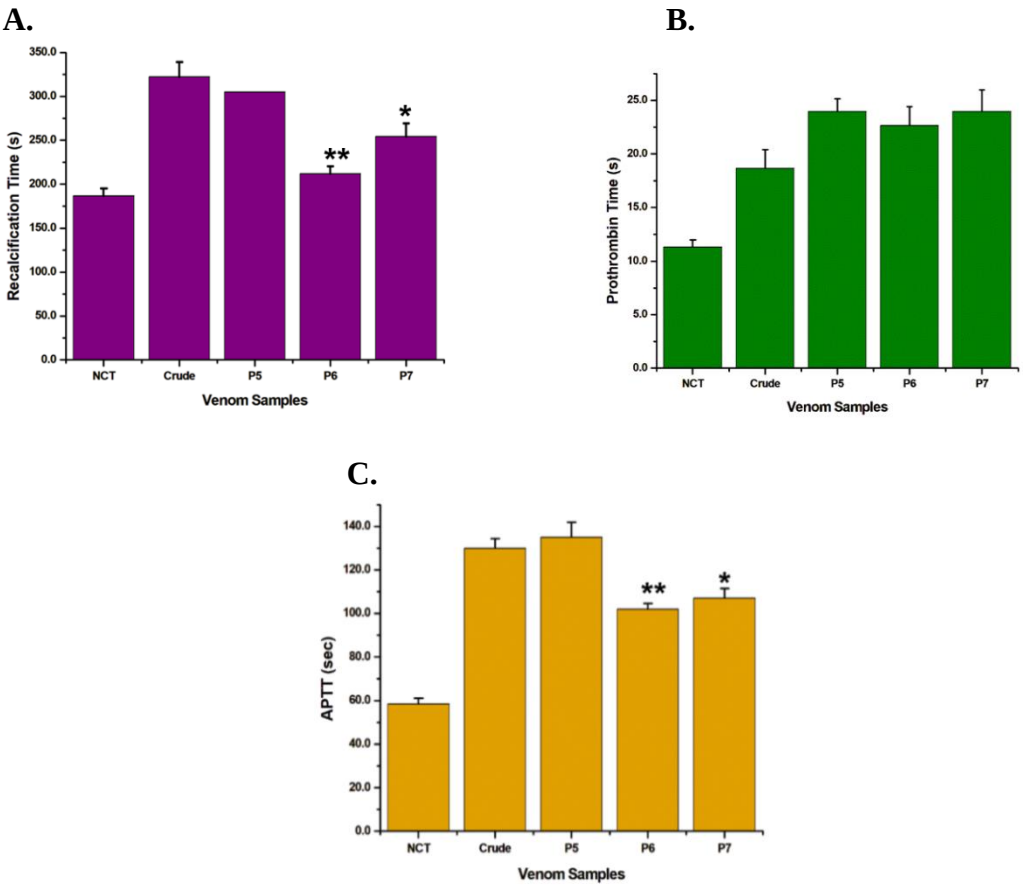

Figure 5.2: Determination of anticoagulant activity of *B. fasciatus* venom and poorly-immunodepleted P5, P6 and P7 peaks. (A) RT, **(B)** PT, and **(C)** APTT. Time needed for PPP to clot after addition of 20 mM Tris-Cl buffer (pH 7.4) is depicted by the NCT. Each bar depicts the mean ± S.E of three experiments. The significance level ($^{\#}p$<0.001, **p<0.01, and *p<0.05) is in relation to the crude venom.

5.3.2 Neutralization of in vitro enzymatic activities

In vitro neutralization studies of enzymatic activities were carried out by pre-incubating the venom with the Premium Serum polyvalent antivenom at 1:100 ratio. The sPLA$_2$ activity of *B. fasciatus* venom and the peaks without incubation with polyvalent antivenom was considered 100%. In sPLA$_2$ neutralization activity, moderate neutralization was observed for P7 (49.9%) and P5 (43.1%), however, no neutralization was observed for P6. During RT, the highest inhibition was observed for crude (37.5%) followed by P5 (37.3%), P7 (24.7%) and P6 (7.3%) respectively. For PT, the highest

inhibition was for P5 (25.0%), followed by crude (21.4%), P6 (11.8%) and P7 (8.3%). The highest inhibition in APTT was demonstrated by crude (55.7%), followed by P5 (44.3%), which was followed by P7 (40.0%) and P6 (39.2%) (Figure 5.3).

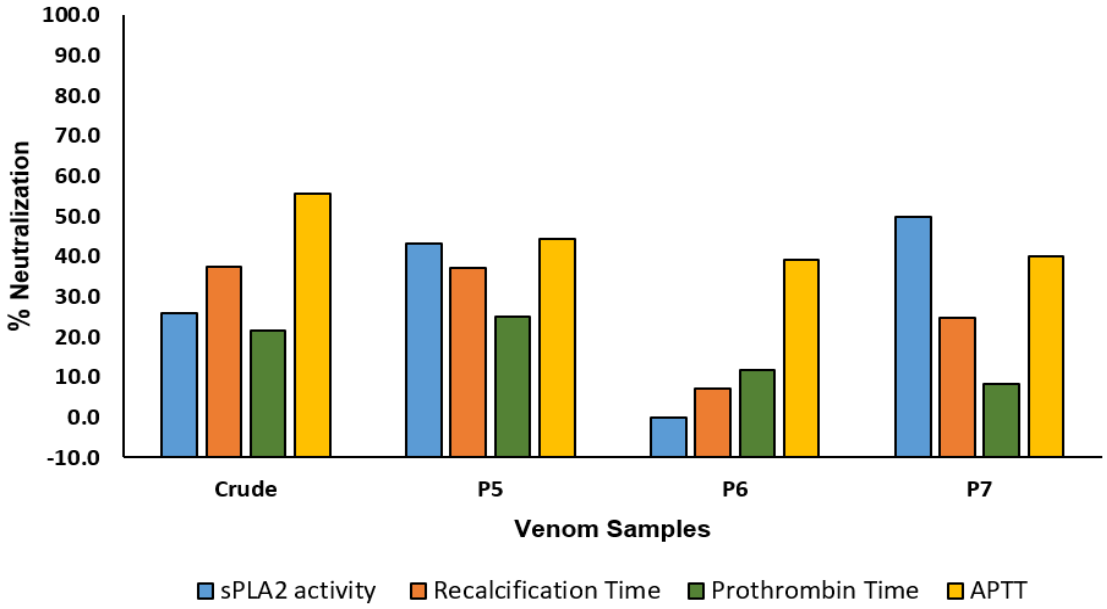

Figure 5.3: In vitro neutralization of enzymatic activities of *B. fasciatus* venom and P5, P6 and P7 peaks by Indian polyvalent antivenom (Premium Serums). A 1:100 ratio of venom-antivenom was pre-incubated for 1 h at 37 ^{o}C before determination of activity. The percent Neutralization was determined by considering the activity without incubation with antivenom as 100%.

5.3.3 Multiple sequence alignment

From the multiple sequence alignment it was observed that the active site residue His-48, and other catalytic residues Asp-49, Asp-99, Tyr-52 and Tyr-73 were conserved for all the identified PLA_2 enzymes. Moreover, the Ca^{2+} binding consensus sequence was conserved between 25 to 33 residues (Y-G-C-Y/F-C-G-X-G-G) for 6 of the 7 PLA_2s except for ABU63161 where Gly-26 was substituted with Ala-26. Moreover, the PLA_2 A6MEY4 had a Cys-19 residue which was not present in any of the other PLA_2s compared (Figure 5.4).

Figure 5.4: Multiple sequence alignment of identified phospholipase A_2 enzymes from poorly-immunodepleted P5, P6 and P7 peaks of *B. fasciatus*. Two PLA_2 (Q6SLM0 and C0HK16) from Big-Four snakes were taken as the control. (The amino acid residues of the identified PLA_2s were obtained after NCBI BLASTp and aligned utilizing DNAMAN X (version 10.3.6.158) programme. The sequences His-48 is depicted in green background. Asp-49, Asp-99, Tyr-52, Tyr-73 and Ca^{2+} binding residues are depicted in blue background. Cys-19 of A6MEY4 is depicted in pink background.

From the percent identity matrix (Table 5.1) obtained after aligning the seven identified PLA_2 proteins from *B. fasciatus* venom, it was observed that six out of the seven proteins (except P0C551) showed high sequence similarity of more than 70% *i.e.*, more than 80 residues. However, the PLA_2 protein P0C551 exhibited less than 52% sequence similarity with the other six identified proteins. From the secondary structure analysis of the proteins showed that the structures were dominated by coils (≥ 61%) followed by alpha-helix ((≥ 24%) and beta-sheets (7-8 %) (Table 5.2).

Table 5.1: Percent identity matrix of seven identified PLA_2 enzymes from *B. fasciatus* venom (Guwahati, Assam).

PLA_2 Accession no.	P0C551	ABU63164	P14411	Q90WA8	ABU63161	Q90WA7	A6MEY4
P0C551	100.0 %	51.3 %	51.7 %	50.8 %	50.0 %	51.7 %	50.0 %
ABU63164	51.3 %	100.0 %	72.6 %	70.9 %	71.8 %	71.8 %	70.9 %
P14411	51.7 %	72.6 %	100.0 %	79.7 %	79.7 %	84.7 %	86.4 %
Q90WA8	50.8 %	70.9 %	79.7 %	100.0 %	91.5 %	89.8 %	88.1 %
ABU63161	50.0 %	71.8 %	79.7 %	91.5 %	100.0 %	88.9 %	88.9 %
Q90WA7	51.7 %	71.8 %	84.7 %	89.8 %	88.9 %	100.0 %	96.6 %
A6MEY4	50.0 %	70.9 %	86.4 %	88.1 %	88.9 %	96.6%	100.0 %

Table 5.2: Comparative analysis of secondary structure of seven identified PLA_2 enzymes from *B. fasciatus* venom (Guwahati, Assam).

PLA_2 Accession no.	**Secondary structural features**		
	Alpha-helix (%)	**Beta-sheet (%)**	**Coils (%)**
P0C551	24	7	69
ABU63164	25	7	68
P14411	25	8	67
Q90WA8	25	8	67
ABU63161	25	8	67
Q90WA7	25	8	67
A6MEY4	31	8	61

5.3.4 Phylogenetic tree analysis

The identified PLA_2s proteins from inadequately immunodepleted P5, P6 and P7 peaks from the venom of *B. fasciatus* were compared to the known PLA_2s from the "Big-Four" venom. From the phylogenetic tree it was observed that six of the seven PLA_2 proteins (except P0C551) from *B. fasciatus* venom clustered together into separate branches to form an evolutionary distinct clade next to the PLA_2s of elapids *B. caeruleus* and *N. naja*. However, one PLA_2 from peak P5 (P0C551) formed a separate branch distant to the other six identified PLA_2s of *B. fasciatus* as well as the PLA_2s of *B. caeruleus* and *Naja naja*. Moreover, all the identified PLA_2s of elapids in Figure 5.5 were evolutionary separated from PLA_2s of the viperids *D. russelii* and *E. carinatus*. The calculated p-distance amounted to 0.10 which indicate a genetic divergence of 0.1% (Figure 5.5).

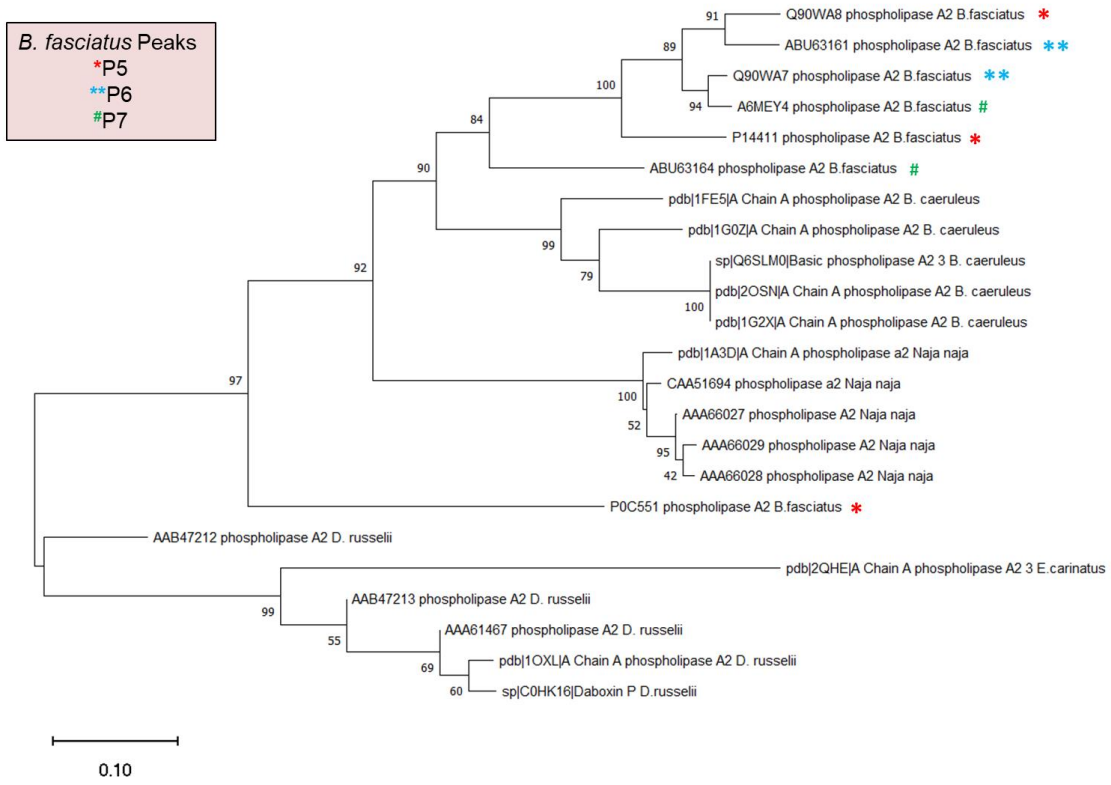

Figure 5.5: Phylogenetic Tree of identified PLA_2 enzymes from *B. fasciatus* (Guwahati, Assam) and known PLA_2 proteins from Indian "Big-Four" snakes. The phylogenetic tree was built by the neighbor-joining method using MEGA software v11.0.

5.3.5 Tertiary structure modelling and validation of identified PLA_2 enzymes

Tertiary structure of the seven identified PLA_2 proteins were modelled in SWISS-MODEL-Expasy server and the ribbon-model structures show three alpha-helices and one beta-wing (consisting of two beta-sheets) between the second and third alpha-helix for each protein. The active site residue His-48 is highlighted in yellow color (ball and stick model) and the Ca^{2+} binding residues (Y25-G-C-Y/F-C-G-X-G-G33) are highlighted in red color. The amino acid Asp49 and Asp99 are highlighted in dark blue, and the residues Tyr52 and Tyr73 are highlighted in pink (Figure 5.6). The modelled structures were validated using Ramachandran plot which demonstrated that ≥90.9% of the residues were in structurally most favoured region and no residues in disallowed region (Figure 5.7). The assessment of the modelled structure's quality were performed using ERRAT 'Overall quality factor' which revealed that all the modelled structure had a good ERRAT score of >95 except P0C551 which had a score of 93.86. Hence, energy minimization of the modelled structure was done using ModRefiner server after which the ERRAT score of P0C551 was raised to 100 (Table 5.3).

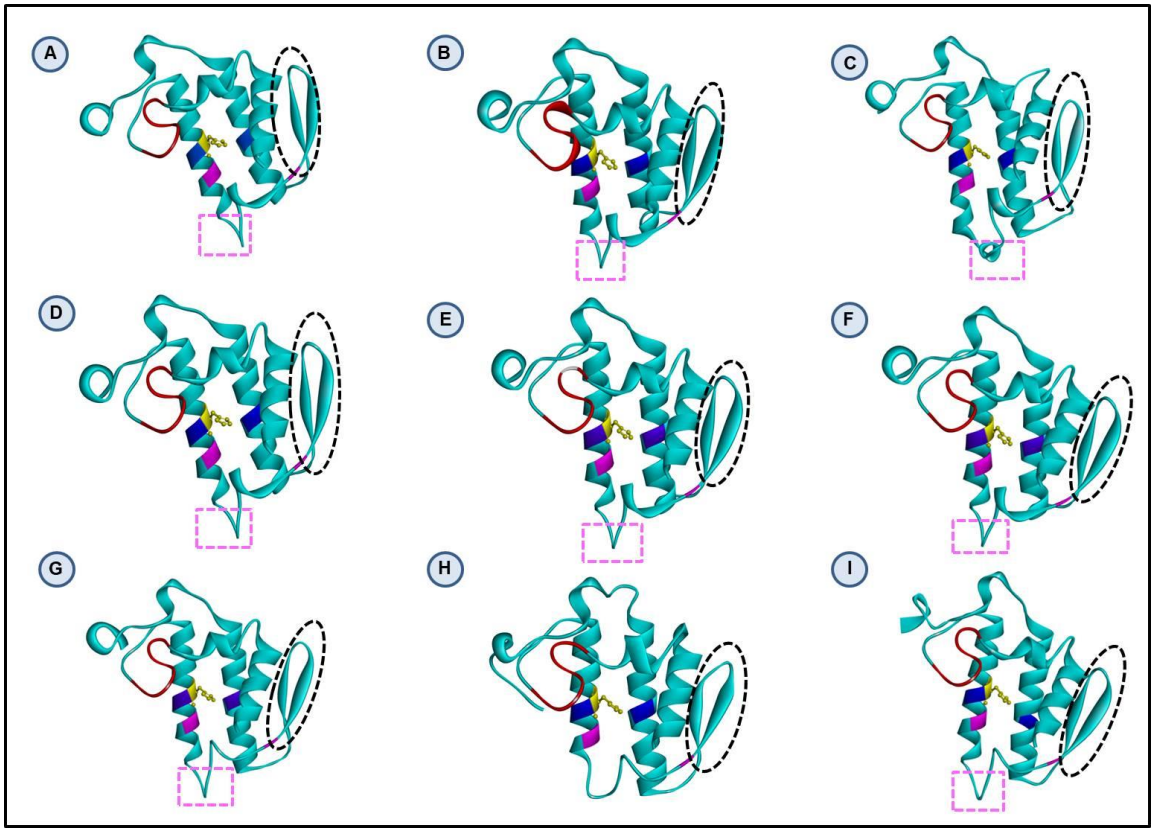

Figure 5.6: Homology modelling and structure prediction of identified PLA_2 enzymes using SWISS-MODEL-Expasy server. Ribbon model of PLA_2 enzymes **(A)** Q90WA8; **(B)** P14411; **(C)** P0C551; **(D)** Q90WA7; **(E)** ABU63161; **(F)** A6MEY4; **(G)** ABU63164; (**H**) C0HK16 (Viperidae: *D. russelii*); (**I**) Q6SLM0 (*B. caeruleus*). Active site residue His-48 is highlighted in purple dotted box (Display style: ball and stick), Asp-49 and Asp-99 are highlighted in dark blue, Tyr-52 and Tyr-73 are highlighted in pink color, and Ca^{2+} binding residues are marked in red color. Ala-26 residue of ABU63161 is highlighted in white color. The characteristic elapid loop (absent in COHK16) is encircled in pink dotted box and the beta-wings are encircled in black dotted circles.

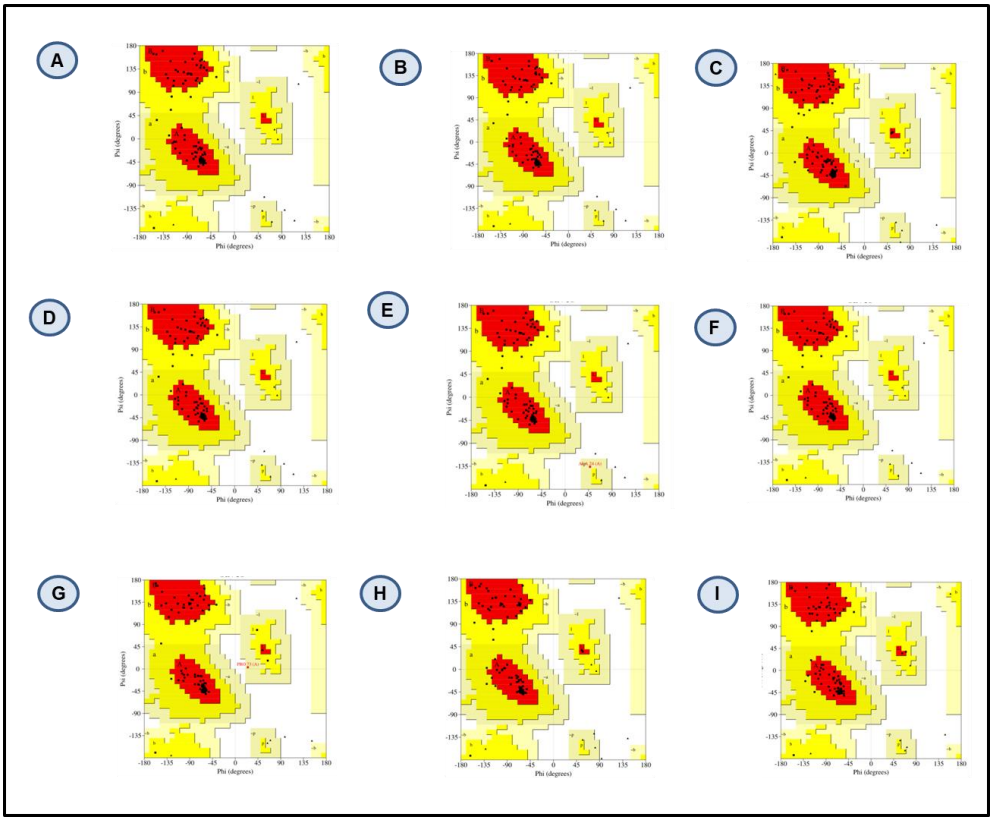

Figure 5.7: Validation of modelled structure of identified PLA_2 enzymes. (A) Q90WA8; **(B)** P14411; **(C)** P0C551; **(D)** Q90WA7; **(E)** ABU63161; **(F)** A6MEY4; **(G)** ABU63164; (**H**) C0HK16 (Viperidae: *D. russelii*); (**I**) Q6SLM0 (*B. caeruleus*).

Table 5.3: Validation of modelled structure by GMQE, MolProbity score, Clash score, Ramachandran plot and ERRAT quality factor.

PLA_2 Uniprot Accession number	**SWISS-MODEL Template ID**	**GMQE**	**Sequence Identity**	**MolProbity score**	**Clash score**	**Ramachandran plot Residues in most favoured + additionally allowed region**	**ERRAT Overall Quality Factor**
Q90WA8	B2KNL1	0.96	91.53%	0.80	0	100%	97.19
P14411	B2KNL1	0.96	79.66%	0.80	0	100%	98.09
P0C551	P0C551	0.93	100%	0.96	0.53	100%	100
Q90WA7	B2KNL1	0.96	88.98	0.99	0.57	100%	95.32
ABU63161	B2KNL1	0.96	100%	0.86	0	99%	97.16
A6MEY4	B2KNL1	0.96	88.98%	0.99	0.57	100%	98.13
ABU63164	P14615	0.96	73.28%	1.23	1.71	100%	96.15
C0HK16	1g2x	0.78	100%	0.86	0	100%	100
Q6SLM0	Q6SLM1	0.96	85.59%	0.92	0.58	100%	95.09

5.3.6 B-cell epitope prediction of identified PLA_2 enzymes

The presence of B-cell epitopes on the identified seven poorly-immunodepleted PLA_2 enzyme's surface was predicted *in silico* and residues with six residues or more were considered for the study. The percent helix of the predicted epitopes was determined by the AGADIR score. Bepipred 2.0 was utilized to predict the linear B-cell epitopes, and four epitopes were identified for enzyme P0C551, and three epitopes each was identified for the remaining six enzymes. Daboxin P from *D. russelii* had four linear epitopes and Q6SLM0 from *B. caeruleus* had three linear epitopes (Table 5.4). The conformational epitopes was predicted in Ellipro server with a minimum score of 0.6, where three epitopes were identified for the enzymes P14411, and four epitopes each was identified for the remaining six enzymes. Daboxin P from *D. russelii* had four conformational epitopes and Q6SLM0 from *B. caeruleus* had five conformational epitopes (Table 5.5). The predicted epitopes were checked for allergenicity using AllerCatPro 2.0 and all the predicted epitopes were identified as non-allergens (except the linear epitope 30-WGGKGTPKDATDRCCF-45 from Daboxin P).

Table 5.4: Prediction of linear B-cell epitopes of seven identified PLA_2 enzymes from the venom of *B. fasciatus* venom using Bepipred 2.0. The allergenicity and helical content of the peptides were calculated using AllerCatPro 2.0 and Agadir tool respectively.

Protein name	Uniprot Accession number	Linear B-cell epitopes	Length	Allergen (A)/Non-Allergen (NA)	Agadir score (% helix)
Basic phospholipase A_2 II	Q90WA8	30-GGTGTPLDELDR-41	12	NA	0.08
		54-KKFGNCIPYF-63	10	NA	0.00
		104-YNLANFGINKE-114	11	NA	0.10
Basic phospholipase A_2 X	P14411	29-KGGSGTPVDQLDRC-42	14	NA	0.14
		56-FGKCNPYFK-64	9	NA	0.00
		104-YNLSNFGINKK-114	11	NA	0.06
Acidic phospholipase A_2 KBf-grIB	P0C551	12-TIPGSFPLLDY-22	11	NA	0.01
		32-GGRGTPVDALDR-43	12	NA	0.10
		58-NPKCSSLLNVPYVK-71	14	NA	0.07
		110-PYKRRNFRIDYK-121	12	NA	0.14

Basic phospholipase A_2 I	Q90WA7	30-GGTGTPLDQLDRC-42	13	NA	0.25
		54-KKFGNCIPYFKT-65	12	NA	0.00
		104-YNLANFGINKE-114	11	NA	0.10
Phospholipase A_2 precursor BFx16	ABU63161	30-GGTGTPLDELDRC-42	13	NA	0.29
		56-FGSCIPYFK-64	9	NA	0.00
		104-YNLANFGIDKE-114	11	NA	0.09
Basic phospholipase A_2	A6MEY4	30-GGTGTPLDQLDR-41	12	NA	0.10
		57-GNCIPYFKT-65	9	NA	0.00
		104-YNLANFGINKE-114	11	NA	0.10
Phospholipase A_2 precursor BFx40	ABU63164	29-YGGSGTPVDELDRC-42	14	NA	0.16
		56-IFKCNPK-62	7	NA	0.00
		104-YNNNNFMMKPK-114	11	NA	0.06
Daboxin P (*D.russelii*)	C0HK16|	12-ETGKLAIPS-20	9	NA	0.01
		30-WGGKGTPKDATDRCCF-45	16	A	0.28
		55-PDCNNKSKRYRY-66	12	NA	0.52
		98-QNLNTYSKKYMLYPDFLCKG-117	20	NA	1.41
Basic phospholipase A2 3 (*B. caeruleus*)	Q6SLM0	29-KGGSGTPVDKLDRC-42	14	NA	0.32
		54-DSIPGCNPNIK-64	11	NA	0.00
		103-PYNINNIMISASN-115	13	NA	0.27

Table 5.5: Prediction of conformational B-cell epitopes of seven identified PLA_2 enzymes from the venom of *B. fasciatus* venom using Ellipro. The allergenicity and helical content of the peptides were calculated using AllerCatPro 2.0 and Agadir tool respectively. An Agadir score of ≥0.13 is highlighted in bold.

Protein name	Uniprot Accession number	Conformational B-cell epitopes	No. of residues	Allergen (A)/Non-Allergen (NA)	ElliPro score	Agadir score (% helix)
Basic phospholipase A_2 II	Q90WA8	T69, C70, N71, K72, P73, D74, T76	7	NA	0.817	0.00
		N52, K54, K55, F56, G57, N58, C59, I60, F63	9	NA	0.815	0.03

		V67, T78, G79, A80, K81, G82, S83	7	NA	0.788	0.01
		K22, G24, C25, Y26, G31, T32, G33, T34, P35, F109, G110, I111, N112, E114, T115, H116, C117, Q118	18	NA	0.657	0.01
Basic phospholipase A_2 X	P14411	T69, C70, N71, K72, P73, N74	6	NA	0.84	0.00
		H51, K54, R55, F56, G57, K58, C59, N60, F63	9	NA	0.814	0.01
		N22, G24, C25, S32, G33, T34, P35, F109, G110, I111, N112, K114, T115, H116, C117	15	NA	0.67	0.02
Acidic phospholipase A_2 KBf-grIB	P0C551	T76, C77, S78, E79, G80, N81, T83	7	NA	0.781	0.01
		N58, P59, K60, C61, S62, S63, L64, L65, N66, V67, V70, K71, S74, S85, A86, D87, N88, D89, E90	19	NA	0.75	**0.42**
		G26, C27, G33, R34, G35, T36, P37, I118, D119, Y120, K121, S122, R123, C124, Q125	15	NA	0.726	**0.38**
		I13, P14, G15, S16, F17, L20	6	NA	0.693	0.00
Basic phospholipase A_2 I	Q90WA7	T69, C70, N71, K72, P73, D74, T76	7	NA	0.818	0.00
		N52, K54, K55, F56, G57, N58, C59, I60, F63	9	NA	0.815	0.03
		E67, T78, D79, A80, K81, G82, S83	7	NA	0.792	0.02
		K22, G24, C25, Y26, G31, T32, G33, T34, P35, F109, G110, I111, N112, E114, T115, H116, C117, Q118	18	NA	0.66	0.01
Phospholipase A_2 precursor BFx16	ABU63161	N52, K54, K55, F56, G57, S58, C59, I60, F63	9	NA	0.814	0.02
		T69, C70, N71, K72, P73, D74, T76	7	NA	0.811	0.00
		E67, T78, D79, A80, K81, G82, S83	7	NA	0.794	0.02
		K22, A24, C25, Y26, G31, T32, G33, T34, P35, L36, D37, E38, A102, P103, F109, G110, I111, D112, K113, E114, K115, H116,	24	NA	0.624	0.11

		C117, Q118				
Basic phospholipase A_2	A6MEY4	T69, C70, N71, K72, P73, D74, T76	7	NA	0.815	0.00
		N52, K54, K55, F56, G57, N58, C59, I60, F63	9	NA	0.81	0.03
		E67, T78, D79, A80, K81, G82, S83	7	NA	0.795	0.02
		K22, G24, C25, Y26, G31, T32, G33, T34, P35, F109, G110, I111, N112, E114, T115, H116, C117, Q118	18	NA	0.656	0.01
Phospholipase A_2 precursor BFx40	ABU63164	T69, C70, N71, K72, P73, D74	6	NA	0.848	0.00
		S67, T78, D79, A80, K81, G82, T83	7	NA	0.755	0.01
		G24, C25, Y26, G31, S32, G33, T34, P35, M111, K112, P113, K114, T115, H116, C117	15	NA	0.682	0.00
		N1, E54, I56, F57, C59, N60, P61, T63, K64	10	NA	0.607	0.16
Daboxin P (*D.russelii*)	C0HK16	R65, K67, K68, V69, N70, G71, A72, V74, E76	9	NA	0.823	0.00
		C26, G32, K33, G34, T35, P36, K37, Y110, P111, D112, F113, L114, C115, K116, G117, E118, L119, V120, C121	19	NA	0.694	0.10
		S1, L54, P55, D56, C57, N58, N59, S61, K62, R63, Y64, K77, G78, T79, S80, C81, E82	17	NA	0.682	**0.38**
		S23, Y103, S104, K105, K106, M108, L109	7	NA	0.634	0.06
Basic phospholipase A2 3 (*B. caeruleus*)	Q6SLM0	T69, C70, T71, Q72, P73, N74, T76	7	NA	0.833	0.00
		S67, T78, R79, T80, A81, D82, A83	7	NA	0.772	**0.13**
		N1, D54, S55, I56, P57, G58, C59, N60, P61, N62, I63, K64	12	NA	0.677	0.00
		N22, Y104, N105, I106, N107, I109, M110	7	NA	0.676	0.01
		G24, C25, Y26, G31, S32, G33, T34, P35, I111, S112, A113, S114, N115, S116, C117, Q118	16	NA	0.655	0.08

The 3D structures of two conformational epitopes from PLA_2 P0C551 of *B. fasciatus*, named P0C551_19 (N58, P59, K60, C61, S62, S63, L64, L65, N66, V67, V70, K71, S74, S85, A86, D87, N88, D89, E90) and P0C551_15 (G26, C27, G33, R34, G35, T36, P37, I118, D119, Y120, K121, S122, R123, C124, Q125), with Agadir scores of 0.42 and 0.38 respectively, are compared with an epitope on Daboxin P named C0HK16_17 (S1, L54, P55, D56, C57, N58, N59, S61, K62, R63, Y64, K77, G78, T79, S80, C81, E82) with Agadir score of 0.38, and another epitope on Q6SLMO from *B. caeruleus* named Q6SLM0_7 (S67, T78, R79, T80, A81, D82, A83) with Agadir score of 0.13. Although the location of epitope P0C551_19 may seem to partially overlap the location of epitopes COHK16_17 and Q6SLM0_7 on their respective PLA_2s, however, the amino acid residues forming the epitopes are completely different. The epitope P0C551_15 (*B. fasciatus*) is located at a site different from the other three epitopes and also involves three residues of the Ca^{2+} binding site (G26, C27, G33) (Figure 5.8).

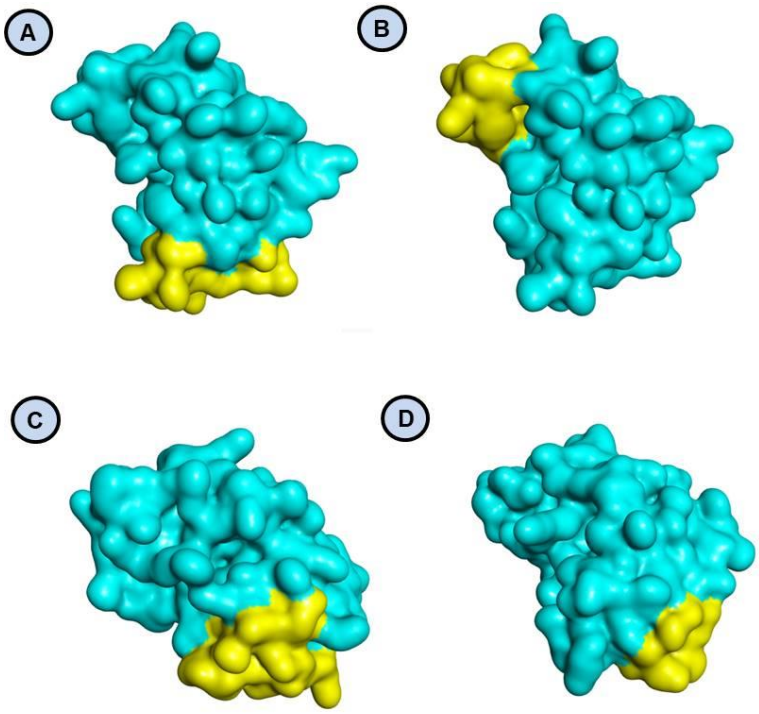

Figure 5.8: Predicted tertiary structure of Conformational B-cell epitopes (Ball structure) on surface structure of PLA_2 enzyme (P0C551) and Positive controls from "Big-Four" snakes. A. P0C551_19 (Agadir score 0.42); **B.** P0C551_15 (Agadir score 0.38); **C.** C0HK16_17 (*D. russelii*) (Agadir score 0.38); **D.** Q6SLM0_7 (*B. caeruleus*) (Agadir score 0.13).

5.3.7 Surface cavity search in identified PLA_2 enzymes

The surface cavity search in the seven identified PLA_2 enzymes from *B. fasciatus* venom using CASTp 3.0 webserver revealed the presence of surface cavity in all the enzymes (Figure 5.9).

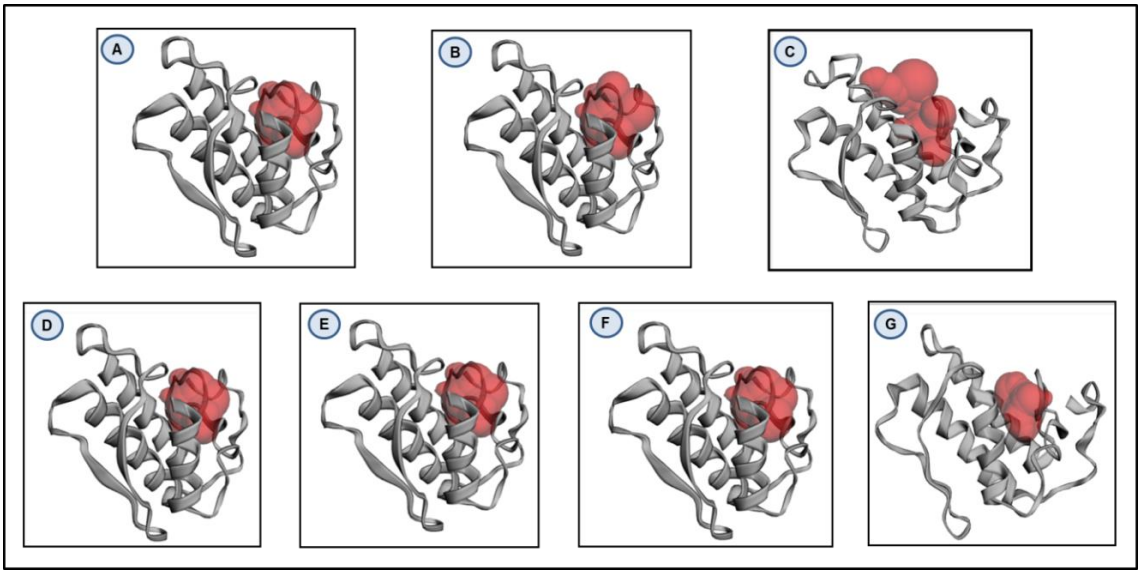

Figure 5.9: Predicted surface cavity of identified PLA_2 enzymes from *B. fasciatus* venom (Guwahati, Assam) using CASTp 3.0 webserver. PLA_2 accession number **(A)** Q90WA8; **(B)** P14411; **(C)** P0C551; **(D)** Q90WA7; **(E)** ABU63161; **(F)** A6MEY4; **(G)** ABU63164.The predicted surface pocket is depicted in red colored spheres.

Table 5.6: Area and Volume of predicted surface cavity in identified PLA_2 enzymes, and their vicinity to active and/or Ca^{2+}-binding sites.

PLA_2 Accession no.	**Area ($Å^2$)**	**Volume ($Å^3$)**	**Vicinity to active site**	**Vicinity to Ca^{2+}-binding site**
Q90WA8	198.68	133.31	Yes	Yes
P14411	233.19	165.79	Yes	Yes
P0C551	330.64	211.36	Yes	Yes
Q90WA7	198.75	133.28	Yes	Yes
ABU63161	198.91	133.27	Yes	Yes
A6MEY4	190.61	135.49	Yes	Yes
ABU63164	201.82	127.33	Yes	Yes

The largest cavity in terms of volume ($Å^3$) was observed in P0C551 (211.36 $Å^3$) and the smallest cavity was observed in ABU63164 (127.33 $Å^3$). The vicinity of the active site from the surface cavity and/or Ca^{2+} binding sites was also analysed. It was observed that the surface cavity of all the identified PLA_2 enzymes were located in vicinity of the active site as well as the Ca^{2+} binding sites (Table 5.6).

5.4 Discussion

In the previous chapter the inadequately immunodepleted venom toxins were determined as PLA_2 proteins, and in this chapter the enzymatic activities of these proteins followed by their neutralization by polyvalent antivenom (Premium Serums) was studied in vitro.

From the PLA_2 activity assay, it was observed that the PLA_2 activity was evident in all the three peaks, although at a reduced level in comparison to the crude venom of *B. fasciatus*. Further, in the coagulation assays (RT, PT and APTT) using PPP from goat plasma, it was observed that the PLA_2 proteins (P5, P6 and P7 peaks) impact both the intrinsic and extrinsic blood coagulation pathways. The PLA_2 and anti-coagulant activity correlates to the identification of PLA_2 enzymes in the crude *B. fasciatus* venom by LC-MS/MS analysis. Previous studies have also reported anti-coagulant properties of *B. fasciatus* crude venom and isolated proteins from the venom. For example, Basic phospholipase A2 VI (Uniprot ID P00627) containing 118 residues was the first PLA_2 enzyme isolated from the venom of *B. fasciatus* which was reported to have anti-coagulant activity in APTT test [171]. Moreover, the BF-AC1 and BF-AC2 proteins also identified from the venom of *B. fasciatus* exhibited anti-coagulant properties in vitro. These proteins have structural and functional similarity with β-Bungarotoxins with a larger subunit (corresponding to PLA_2) and a smaller subunit (corresponding to Kunitz-type serine protease inhibitor (KSPI)), and the anti-coagulant activity is dependent on the extent of enzymatic activity exhibited by the PLA_2 subunit [172]. Victims envenomated by *B. fasciatus* venom have also reported delay in clotting time [39] which may be attributed to the presence of high amounts of PLA_2 proteins.

Neutralization of the enzymatic activities using polyvalent antivenom (Premium Serums) in vitro revealed insufficient and poor inhibition of the PLA_2 and anti-coagulant activities exhibited by the venom of *B. fasciatus* and P5, P6 and P7 peaks. These findings are also supported by the results of the 3G antivenomics study mentioned in chapter 4.

Previously, a binding study using the venom of *B. fasciatus* from West Bengal, India against four polyvalent antivenom (Premium Serums and Vaccines Ltd., Vins Bioproducts Ltd., Bharat Serums and Vaccines Ltd., and Haffkine Institute) manufactured in India, revealed that the binding effectiveness for Premium Serums was the lowest (1:100 effective dilution) while the other three antivenom had a relatively high effective dilution (1:500) [78]. On the other hand, in another study by Hia et al., monovalent antivenom (BFMAV) was utilized against the venom of *B. fasciatus* and had proved to be effective. The BFMAV was raised targeting the venom of *B. fasciatus* from Thailand against which it had maximum neutralization potency, however, the potency gradually lowered when the venom of *B. fasciatus* from other countries such as Myanmar, Indonesia, China and Malaysia were tested [58]. This suggests that venom variation due to geographical variations may affect the neutralization potency of monovalent antivenom. However, in India, the non-production of monovalent antivenom specific to the venom of *B. fasciatus* along with poor efficacy of Indian polyvalent antivenom serves as a disadvantage and makes it challenging for health care providers for treating victims envenomated by *B. fasciatus*.

The PLA_2 enzymes obtained in this study were characterized *in silico* and compared to two basic PLA_2 enzymes (eg. Basic phospholipase A2 3 (Q6SLM0) from *B. caeruleus* and Daboxin P (C0HK16) from *Daboia russelii*) which are representatives of the "Big-Four" snakes. From the Multiple Sequence Alignment, it was observed that some of the residues were conserved for all the identified PLA_2 enzymes. The Histidine (H) residue at the active site *i.e.,* 48^{th} position (His-48) plays a crucial role in the PLA_2 activity and if this residue is alkylated it may result in loss of enzymatic activity [231]. The His-48 residue of PLA_2 proteins identified in this study are conserved which indicate that these proteins might be enzymatically active. Other than His-48, the presence of Asp99, Tyr52 and Tyr73 are also responsible for the construction of the catalytic framework and these three residues are also conserved in all the seven identified PLA_2s. The oxygen atom of residue Asp49 is also important for catalysis whose substitution by other residue leads to loss of Ca^{2+} binding activity, and Asp49 is also conserved in all the identified PLA_2s. Moreover, the Ca^{2+} binding residues was conserved from 25^{th} to 33^{rd} position (Y-G-C-Y/F-C-G-X-G-G) for 6 of the seven PLA_2 enzymes except for ABU63161 where Gly-26 was substituted with Ala-26. However. four of the seven identified PLA_2 enzymes (Uniprot ID Q90WA7, Q90WA8, ABU63161 and A6MEY4) contain a Proline residue at

31st position, which are also known as P31-PLAs (Table 4.5). These proteins have activity (modulation of calcium-dependent potassium channels and muscle fibre damage) similar to cytotoxins (CTX) from cobra venom and are reported to be moderately lethal [27,256]. These P31-PLAs have also been studied previously by Tsai et al. in the venom of *B. fasciatus* from Eastern India [27] and other elapid venoms from *Laticauda colubrina*, *Pseudechis porphyriacus* and *P. australis* [257–259]. The catalytic activity of elapid venom with high P31-PLA content has been found to be similar in function to viperid venom with K49-PLAs reported from viperid venom such as *Trimerusurus sp.* [27]. These basic P31-PLAs and K49-PLAs occur in high proportions in the venom, although catalytic activity is not present. They retain their capacity to attach to interface or membranes resulting in pathophysiological implications in bite victims like myotoxicity, cytotoxicity, hyperalgesia and edema [260,261]. A Cys-19 residue was present in the A6MEY4 PLA_2 which suggests the formation of interchain by the residue which may play a role in formation of disulphide bonds with other Cys residues or may co-ordinate the binding of calcium ion in the active site of the enzyme.

Elapid snakes which contain PLAs with Lysine (K), Leucine (L), or Arginine (R) residues at 31st position are mostly basic and have a high catalytic activity [262,263]. The position is critical for interface identification which is located anterior to the substrate binding site and removal of this residue may inhibit the calcium binding property and its overall stability [264,265]. A K31-PLA protein (Uniprot ID P14411), which has been identified in this study in the venom sample of *B. fasciatus*, may be catalytically active (Table 4.5). Further, *in silico* and in vitro study of these identified proteins would provide more insights into the functional properties of these PLA_2 enzymes.

The percent identity matrix obtained from Multiple Sequence Alignment shows that six of the PLA_2 enzymes share > 70% homology, however, the PLA_2 P0C551 has a lower homology of <52% (Table 5.1). Minor difference in the secondary structure (percentage of alpha-helices, beta-sheets and coils) of the identified PLA_2s have also been observed, where interestingly, P0C551 has the lowest percentage of alpha-helix (24%) and the highest percentage of coils (69%) compared to the other six PLA_2s (Table 5.2). Further, the phylogenetic tree analysis (Figure 5.5) revealed that six of the PLA_2 proteins of *B. fasciatus* have a closer evolutionary kinship with the PLA_2 proteins of *B. caeruleus*

followed by that of *N. naja*. Due to this evolutionary closeness the antibodies of the polyvalent antivenom can exhibit certain level of cross-neutralization towards the venom proteins of *B. fasciatus* as well. However, the distant evolutionary relation of PLA_2 P0C551 to the PLA_2s from "Big-Four" snakes indicates that antibodies which are raised against the venom proteins (PLA_2s in this case) of "Big-Four" snakes in hyperimmunized horses may not be effective in binding this particular PLA_2 enzyme.

The PLA_2 enzymes present in elapids and mammalian pancreas belong to Group I PLA_2s (~13-14 kDa) which is characterized by the presence of 115-133 amino acids and 7 disulfide bridges with a characteristic disulphide bridge between Cys11 and Cys77 residue. This group of snake venom PLA_2s have a typical loop on their surface known as the elapid loop, connecting the catalytic alpha-helix to the beta-wing. The Group 1 PLA_2s are subdivided into Group 1A or Group 1B depending on the presence of the elapid loop or the mammalian pancreatic loop (residues 62-67) respectively. The PLA_2 enzymes typically have 3 alpha-helices and 2 antiparallel beta-sheets bound together due to disulphide bonds. The His-48 of the active site, N-terminal helix, antiparallel-helix, Ca^{2+} binding loop and beta-wing remain conserved [237]. In this study, tertiary structure modelling using *in silico* approach exhibited all the characteristic structural features for the seven identified PLA_2 enzymes as well as the Q6SLM0 from *B. caeruleus*. The characteristic elapid loop is absent in Daboxin P from the viperid *Daboia russelii* as it belongs to Group II PLA_2s.

There is an increasing demand for the development of novel and more superior antivenom against medically important snake species of biodiversity rich regions such as North-East India. Although the proteomics based 'antivenomics' approach (previously described in chapter 4) provide crucial information on venom fractions recognized by a particular antivenom as well as the para-specificity of the antivenom, however, it does not provide much information on the molecular interactions between the venom toxins and the antivenom which is the basis of the observed para-specificity [266,267]. Computational methods can be explored to understand these interactions and toxin specific antibodies can then be designed, synthesized and studied for biological experiments. In this study, the B-cell epitopes present on the surface of identified PLA_2 enzymes are predicted and compared with those present on the surface of Q6SLM0 (*B. caeruleus*) and Daboxin P (*Daboia russelii*) using *in silico* approach. All the predicted

linear and conformational B-cell epitopes were non-allergens (except a 15-residue linear epitope on Daboxin P). The protein secondary structure of these monomeric epitopes which is mainly dependent on the helical content was determined by the AGADIR tool. Comparison of the linear and conformational B-epitopes on PLA_2s from *B. fasciatus* with that of *B. caeruleus* (Q6SLM0) and *D. russelii* (Daboxin P) exhibits differences in their sequences as well as in their relative location on the molecule (Figure 5.8), which may be responsible for poor-immunodepletion of these enzymes by Indian polyvalent antivenom. Further *in silico* studies into the binding of these epitopes to IgG molecules or their fragments, and stability of these interactions using molecular dynamics simulation, followed by in vitro and in vivo experiments is required to validate the findings of this study. Recently, Grahadi et al. have predicted epitopes present on candoxin protein from *Bungarus candidus* venom, prevalent in South-East Asia, using an *in silico* approach and identified a non-allergic 15-mer epitope (47-CFKESWREARGTRIE-61) which has the best binding efficiency to the active site of murine and human major histocompatibility complex (MHC) Class II, and further molecular dynamics study showed that the epitope was stable [268]. Similarly, Hiu et al. have reported B-cell and T-cell epitopes from a conserved cytotoxin from *Naja* venom using *in silico* and in vitro approach. Four potential epitopes located at the functionally active loop of Cytotoxin was identified using different epitope mapping approaches which are critical for the folding and toxicity of CTX [269]. Moreover, Ashraf et al. have also previously utilized an *in silico* approach to identify epitope sequences on alpha-delta-bungarotoxin-4 from the "Big-Four" snake *B. caeruleus.* Two non-allergic epitopes (GENLCYTKM and FCSSRGKVI), which bound to MHC Class I and Class II peptides, were determined which could potentially elicit an immune response [270]. Interestingly, a proof-of-concept study for toxin-targeted antivenom was exhibited by Wagstaff et al. where they designed and developed a string antiserum against a synthetic DNA immunogen, with seven epitopes (epitope string). It specifically targeted venom metalloproteases from *Echis ocellatus*, and could neutralize hemorrhage by *E. ocellatus* as well as other African viper venoms [271].

Surface cavity search was performed for all the seven identified PLA_2 enzymes identified in this study to explore the possibility of inhibitors (such as small synthetic inhibitors and aptamers) to bind to these pockets and inhibit their function.

From the results (Figure 5.6 and Table 5.9) it is evident that surface cavity in the vicinity of the active site as well as the Ca^{2+} binding site are present for all the seven PLA_2 enzymes. Recently, from our lab, Devi et al. reported from an *in silico* analysis, three plant based molecules namely butein (-8.2 kcal/mol), bakuchiol (-7.9 kcal/mol) and mimosine (-5.7 kcal/mol) to bind to the surface pocket of the modelled structure of the PLA_2 enzyme Daboxin P (from *Daboia russelii* venom) with high binding efficiency. While butein interacted with the active site residues, bakuchiol and mimosine engaged with the Calcium-binding residues, and validation of enzymatic inhibition was also exhibited in vitro by the inhibition of $sPLA_2$ activity [272]. Further, using *in silico* approaches such as molecular docking, inhibitors fitting the surface cavities identified in this study can be screened; also new inhibitors can be developed to inhibit the active site or the Calcium-binding site of the PLA_2 enzymes.

5.5 Conclusion

In this chapter, the poorly-immunodepleted PLA_2 enzymes have been characterized for their enzymatic activities in vitro which exhibited PLA_2 and anti-coagulant activities. Subsequent neutralization by Indian polyvalent antivenom have demonstrated moderate to poor neutralization of these activities. Multiple sequence alignment have revealed that the active site residues are conserved for all the seven PLA_2 enzymes and the Ca^{2+} binding residues are conserved for six of the enzymes (except for ABU63161). The phylogenetic tree showcased the evolutionary closeness of six of the PLA_2 enzymes with that of the elapids of "Big-Four" snakes, except for P0C551, which was distantly related to the others. Tertiary structure modelling of the PLA_2 enzymes revealed that the three alpha-helices, beta-wings and the elapid loop are conserved in all the enzymes. Linear and conformational non-allergic B-cell epitopes identified on the PLA_2 enzyme surfaces can be utilized to understand venom-antivenom interactions and to develop toxin-specific antivenom. Furthermore, surface cavities identified on the PLA_2 enzymes in close vicinity of the active site or allosteric sites may help to study potential binding with inhibitors or to design new inhibitors.